

Contribution from the Departments of Chemistry, Texas A&M University, College Station, Texas 77843, and University of Natal, Pietermaritzburg, Natal, South Africa

Structural and Dynamic Study of Bis(tetraethyl pyrophosphite)pentacarbonyliron(Fe-Fe) and (Tetraethyl pyrophosphite)heptacarbonyliron(Fe-Fe)

F. ALBERT COTTON,*^{1a} RAYMOND J. HAINES,^{1b} BRIAN E. HANSON,^{1a} and JANINE C. SEKUTOWSKI^{1a}

Received December 5, 1977

The dynamic behavior of $[(C_2H_5O)_2POP(OC_2H_5)_2]_2Fe_2(CO)_5$ and $[(C_2H_5O)_2POP(OC_2H_5)_2]Fe_2(CO)_7$ has been studied by carbon-13 NMR spectroscopy. Only one CO-exchange process is seen in $(POP)_2Fe_2(CO)_5$, where $(C_2H_5O)_2POP(OC_2H_5)_2$ is represented by POP. This process exchanges all five CO's via a concerted, cyclic movement of the five CO groups. In $(POP)Fe_2(CO)_7$ there are two CO-exchange processes. The first is the same as that observed for $(POP)_2Fe_2(CO)_5$ and exchanges five CO's while a second process involving local exchange on each Fe atom combines with the first to cause complete scrambling of all seven CO's. The crystal structure of $(POP)_2Fe_2(CO)_5$ has been determined by X-ray crystallography. It crystallizes in space group $P\bar{1}$ with $a = 17.850(5)$ Å, $b = 18.082(6)$ Å, $c = 11.270(2)$ Å, $\alpha = 97.26(2)^\circ$, $\beta = 97.21(2)^\circ$, $\gamma = 102.69(2)^\circ$, and $Z = 4$. There are two independent molecules per asymmetric unit in which the Fe-Fe bond lengths are 2.663(2) and 2.669(2) Å.

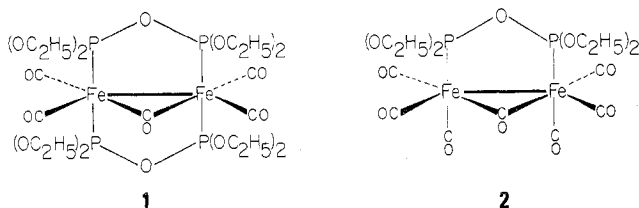
Introduction

Carbonyl scrambling in molecules of the type $(L-L)Fe_2(CO)_7$ ($L-L$ = bridging bidentate ligand) has received relatively little attention compared to studies of other dinuclear metal carbonyl compounds. Only two molecules of this type have been studied by dynamic carbon-13 NMR, namely, $(Ph_2PCH_2PPh_2)Fe_2(CO)_7$ ² and $(1,2-C_4H_4N_2)Fe_2(CO)_7$.³ The former compound is undergoing CO exchange rapidly and thus shows a sharp 1:3:1 triplet even at $-110^\circ C$. No mechanistic information was obtainable. Mechanistic information was obtained from the study of $(1,2-C_4H_4N_2)Fe_2(CO)_7$ where it is clear that two distinct CO-exchange processes occur. One involves internuclear scrambling of the five approximately coplanar CO groups and the other is presumably local exchange of the three terminal CO groups on each iron atom.

Structural and dynamic studies have now been done on the tetraethyl pyrophosphite (POP) derivatives⁴ of $Fe_2(CO)_9$, $(POP)_2Fe_2(CO)_5$, **1**, and $(POP)Fe_2(CO)_7$, **2**, for comparison with previous results. These studies are fully reported in this paper.

Experimental Section

Carbon-13 NMR Measurements. These were made on a JEOL PFT 100/Nicolet 1080 Fourier transform spectrometer operating at 25.037 MHz. Spectra for $(POP)_2Fe_2(CO)_5$, **1**, and $(POP)Fe_2(CO)_7$, **2**, were obtained on samples containing ¹³CO at natural abundance.



Approximately 12 mg of $Cr(acac)_3$ was added to each sample. For both compounds the following solvent systems were used: above -45° , $CDCl_3$ and 5% Me_4Si ; below -45° , 30% CD_2Cl_2 , 30% C_2H_5Cl , 35% $CHCl_3$, and 5% Me_4Si . Chemical shifts were measured from Me_4Si . In $(POP)_2Fe_2(CO)_5$, $J_{31P-13C} = 19.8$ Hz at $-40^\circ C$ and in $(POP)Fe_2(CO)_7$, $J_{31P-13C} = 6.0$ Hz at $0^\circ C$.

X-ray Structure Determination for 1. The procedure for X-ray data collection has been described previously.³ The crystal was found to be triclinic, space group $P\bar{1}$, with the following unit cell dimensions: $a = 17.850(5)$ Å, $b = 18.082(6)$ Å, $c = 11.270(2)$ Å, $\alpha = 97.26(2)^\circ$, $\beta = 97.21(2)^\circ$, $\gamma = 102.69(2)^\circ$, and $Z = 4$, with two independent molecules per asymmetric unit. Data were collected in the range $0 < 2\theta \leq 45^\circ$ using Mo $K\alpha$ radiation. Of 5657 reflections, 3154 had $I > 3\sigma$ and were used as observed data.

Software provided by Enraf-Nonius was used to solve and refine the structure on a PDP 11/45 computer.⁵ Four iron atoms and eight

phosphorus atoms were located from an E map obtained using the phase set with the highest figure of merit generated by the program MULTAN. To do this, 492 reflections with E values greater than 1.75 were used. The remaining nonhydrogen atoms were found by conventional difference Fourier techniques alternated with least-squares refinement cycles. Refinement converged with anisotropic thermal parameters for the Fe and P atoms giving discrepancy indices of $R_1 = 0.088$ and $R_2 = 0.110$ and the error in an observation of unit weight of 2.38. A table of calculated and observed structure factors is available as supplementary material.

Results

The molecular structure of **1** is shown in Figure 1 and the positional and thermal vibration parameters are listed in Table I. Bond lengths and bond angles are given in Tables II and III. For simplicity only the atoms of molecule **1** are listed by number. Iron atoms Fe(3) and Fe(4) of molecule **2** correspond to Fe(1) and Fe(2) of molecule **1**, and phosphorus atoms $P(n+4)$, oxygen atoms $O(n+15)$, and carbon atoms $C(n+21)$ of molecule **2** correspond to $P(n)$, $O(n)$, and $C(n)$ of molecule **1**. Table IV lists some important least-squares planes.

The variable-temperature carbon-13 NMR spectra for **1** are shown in Figure 2 while Figure 3 shows the spectra for **2**.

Discussion

Molecular Structure of 1. The molecule $(POP)_2Fe_2(CO)_5$ is an extension of the structural type previously observed for $(Ph_2PCH_2PPh_2)Fe_2(CO)_7$ ² and $(1,2-C_4H_4N_2)Fe_2(CO)_7$,³ in which two additional CO groups, trans to the ligating atoms of the first ligand, have been replaced by a second bridging bidentate ligand. The two POP ligands in **1** thus occupy positions trans to each other and the four phosphorus atoms define a plane (see Table IV) containing the two iron atoms.

There is a slight twisting of each Fe-Fe-P-O-P ring as seen from the distances for plane 1 in Table IV. The $Fe_2(CO)_5$ unit forms a plane that is perpendicular to the plane defined by the Fe_2P_4 unit. The $Fe_2(CO)_5$ moiety contains one bridging CO and two different types of terminal CO groups.

The Fe-Fe bond length in **1**, averaged for the two molecules, is 2.666(2) Å, only slightly shorter than that in $(Ph_2PCH_2PPh_2)Fe_2(CO)_7$ which has an Fe-Fe distance of 2.709(2) Å. In **1** the P-P separation is 2.82(3) Å whereas in the $(Ph_2PCH_2PPh_2)$ compound the P-P separation is 3.00(4) Å. The compression of the Fe-Fe bond in **1** may well be due to the shorter "bite" of the POP ligand.

A direct structural comparison of the bonding of phosphine and phosphite ligands was first made by Grimm and co-workers for $Ph_3PCr(CO)_5$ and $(PhO)_3PCr(CO)_5$.⁶ It was

Table I. Positional and Thermal Parameters and Their Estimated Standard Deviations^a

Atom	x	y	z	β_{11}	β_{22}	β_{33}	β_{12}	β_{13}	β_{23}
Fe(1)	0.7687 (2)	0.2846 (1)	0.3687 (2)	0.0037 (2)	0.00347 (8)	0.0069 (2)	0.0007 (2)	0.0017 (3)	0.0002 (2)
Fe(2)	0.7053 (2)	0.1929 (1)	0.5151 (2)	0.0041 (2)	0.00379 (8)	0.0081 (2)	0.0026 (2)	0.0025 (3)	0.0032 (2)
Fe(3)	0.7319 (2)	0.6985 (1)	0.0592 (2)	0.0035 (2)	0.00332 (8)	0.0078 (2)	0.0019 (2)	0.0019 (3)	0.0023 (2)
Fe(4)	0.8029 (2)	0.7808 (1)	-0.0931 (2)	0.0031 (2)	0.00366 (8)	0.0074 (2)	0.0015 (2)	0.0017 (3)	0.0018 (2)
P(1)	0.7490 (4)	0.3852 (3)	0.4722 (4)	0.0048 (4)	0.0036 (2)	0.0099 (4)	0.0007 (4)	0.0021 (6)	0.0012 (5)
P(2)	0.6889 (3)	0.2893 (3)	0.6330 (4)	0.0041 (4)	0.0049 (2)	0.0065 (3)	0.0025 (4)	0.0024 (5)	0.0011 (4)
P(3)	0.7821 (3)	0.1883 (3)	0.2476 (4)	0.0048 (4)	0.0043 (2)	0.0081 (4)	0.0020 (4)	0.0039 (6)	0.0004 (5)
P(4)	0.7068 (4)	0.0923 (3)	0.3950 (5)	0.0053 (4)	0.0040 (2)	0.0144 (5)	0.0036 (4)	0.0063 (7)	0.0033 (5)
P(5)	0.8423 (4)	0.7125 (3)	0.1737 (4)	0.0045 (4)	0.0045 (2)	0.0097 (4)	0.0025 (4)	0.0010 (6)	0.0053 (4)
P(6)	0.9172 (4)	0.7882 (3)	0.0015 (4)	0.0047 (4)	0.0054 (2)	0.0094 (4)	0.0028 (4)	0.0022 (6)	0.0035 (5)
P(7)	0.6200 (3)	0.6757 (2)	-0.0534 (4)	0.0038 (4)	0.0036 (2)	0.0086 (4)	0.0019 (4)	0.0018 (6)	0.0020 (4)
P(8)	0.6942 (3)	0.7683 (2)	-0.2106 (4)	0.0033 (3)	0.0037 (2)	0.0075 (4)	0.0012 (4)	-0.0003 (6)	0.0014 (4)
Atom	x	y	z	$B_{iso}, \text{\AA}^2$	Atom	x	y	z	$B_{iso}, \text{\AA}^2$
O(1)	0.6973 (7)	0.3696 (6)	0.5812 (9)	5.0 (3)	O(16)	0.9206 (7)	0.7454 (6)	0.1207 (9)	5.4 (3)
O(2)	0.7464 (7)	0.1035 (6)	0.2740 (9)	5.1 (3)	O(17)	0.6186 (7)	0.7037 (5)	-0.1866 (28)	3.9 (2)
O(3)	0.6009 (7)	0.2233 (6)	0.3183 (9)	5.4 (3)	O(18)	0.7867 (7)	0.6145 (6)	-0.1404 (29)	5.4 (3)
O(4)	0.7601 (9)	0.3640 (7)	0.1647 (12)	8.4 (4)	O(19)	0.6766 (9)	0.5589 (8)	0.1541 (12)	8.8 (4)
O(5)	0.9291 (9)	0.3175 (8)	0.4891 (13)	9.6 (4)	O(20)	0.6960 (9)	0.8231 (7)	0.2144 (11)	7.9 (4)
O(6)	0.8533 (9)	0.1985 (8)	0.6569 (13)	9.8 (4)	O(21)	0.7899 (9)	0.9263 (7)	0.0386 (11)	7.8 (4)
O(7)	0.5820 (9)	0.0989 (8)	0.6081 (12)	9.2 (4)	O(22)	0.8779 (9)	0.8100 (8)	-0.3009 (12)	9.2 (4)
O(8)	0.8274 (8)	0.4438 (7)	0.5383 (11)	7.3 (3)	O(23)	0.8561 (9)	0.7728 (7)	0.2999 (11)	8.1 (4)
O(9)	0.7086 (8)	0.4450 (7)	0.4143 (11)	7.5 (3)	O(24)	0.8669 (10)	0.6449 (8)	0.2315 (13)	10.1 (4)
O(10)	0.7454 (8)	0.3117 (6)	0.7588 (10)	6.6 (3)	O(25)	0.9671 (8)	0.8722 (7)	0.0540 (11)	7.8 (4)
O(11)	0.6077 (7)	0.2859 (6)	0.6769 (9)	5.6 (3)	O(26)	0.9792 (9)	0.7553 (8)	-0.0670 (12)	9.2 (4)
O(12)	0.8644 (8)	0.1791 (7)	0.2226 (11)	7.4 (3)	O(27)	0.6861 (7)	0.7440 (5)	-0.3527 (9)	4.7 (3)
O(13)	0.7436 (8)	0.1834 (6)	0.1092 (10)	6.0 (3)	O(28)	0.6614 (7)	0.8440 (6)	-0.2053 (9)	5.5 (3)
O(14)	0.7561 (10)	0.0354 (9)	0.4389 (13)	10.1 (4)	O(29)	0.5569 (7)	0.7133 (6)	0.0011 (29)	5.0 (3)
O(15)	0.6221 (9)	0.0396 (7)	0.3392 (12)	8.5 (4)	O(30)	0.5677 (7)	0.5906 (6)	-0.0955 (9)	5.4 (3)
C(3)	0.665 (1)	0.2308 (8)	0.375 (1)	4.4 (4)	C(24)	0.775 (1)	0.6716 (8)	-0.084 (1)	3.9 (4)
C(4)	0.764 (1)	0.3307 (10)	0.247 (2)	6.4 (5)	C(25)	0.700 (1)	0.6165 (10)	0.113 (2)	6.5 (5)
C(5)	0.864 (1)	0.3074 (12)	0.435 (2)	8.1 (6)	C(26)	0.708 (1)	0.7727 (10)	0.149 (2)	6.2 (5)
C(6)	0.792 (1)	0.1932 (11)	0.599 (2)	8.2 (6)	C(27)	0.796 (1)	0.8675 (9)	-0.015 (1)	5.6 (4)
C(7)	0.633 (1)	0.1373 (11)	0.569 (2)	7.8 (6)	C(28)	0.847 (1)	0.7977 (10)	-0.215 (2)	6.2 (5)
C(8)	0.830 (2)	0.5190 (14)	0.610 (2)	11.2 (8)	C(29)	0.872 (2)	0.5881 (16)	0.166 (2)	13.2 (9)
C(9)	0.887 (2)	0.5775 (16)	0.559 (3)	14.0 (10)	C(30)	0.947 (2)	0.5638 (18)	0.225 (3)	15.8 (11)
C(10)	0.634 (1)	0.4181 (11)	0.341 (2)	7.4 (6)	C(31)	0.602 (1)	0.5320 (10)	-0.155 (2)	6.9 (5)
C(11)	0.580 (2)	0.4536 (13)	0.409 (2)	10.7 (8)	C(32)	0.542 (1)	0.4546 (13)	-0.157 (2)	9.6 (7)
C(12)	0.741 (1)	0.3800 (12)	0.848 (2)	9.2 (7)	C(33)	0.475 (1)	0.7037 (11)	-0.063 (2)	7.3 (5)
C(13)	0.822 (2)	0.4164 (15)	0.895 (2)	12.3 (9)	C(34)	0.438 (1)	0.7579 (12)	0.002 (2)	9.1 (7)
C(14)	0.533 (1)	0.2708 (11)	0.591 (2)	7.1 (5)	C(35)	0.587 (1)	0.8436 (12)	-0.278 (2)	9.3 (7)
C(15)	0.469 (1)	0.2404 (13)	0.654 (2)	9.6 (7)	C(36)	0.701 (1)	0.6705 (10)	-0.399 (2)	6.0 (5)
C(16)	0.916 (1)	0.1565 (11)	0.309 (2)	7.7 (6)	C(37)	0.716 (1)	0.6770 (12)	-0.530 (2)	8.6 (6)
C(17)	0.924 (1)	0.0755 (13)	0.258 (2)	9.9 (7)	C(38)	0.576 (2)	0.9205 (17)	-0.261 (3)	14.6 (10)
C(18)	0.743 (1)	0.1181 (13)	0.017 (2)	9.5 (7)	C(39)	1.053 (2)	0.8869 (15)	0.113 (2)	12.5 (9)
C(19)	0.717 (2)	0.1344 (14)	-0.102 (2)	11.0 (8)	C(40)	1.079 (2)	0.9698 (13)	0.137 (2)	9.8 (7)
C(20)	0.738 (2)	-0.0007 (20)	0.545 (3)	18.7 (14)	C(41)	0.974 (2)	0.6832 (20)	-0.121 (3)	18.9 (13)
C(21)	0.778 (2)	-0.0657 (15)	0.543 (2)	12.5 (9)	C(42)	1.041 (3)	0.6594 (25)	-0.102 (4)	22.6 (18)
C(22)	0.610 (2)	-0.0359 (15)	0.247 (2)	12.4 (9)	C(43)	0.934 (2)	0.7965 (14)	0.388 (2)	11.1 (8)
C(23)	0.563 (2)	-0.0290 (18)	0.149 (3)	15.9 (11)	C(44)	0.950 (2)	0.8754 (15)	0.412 (2)	12.9 (9)

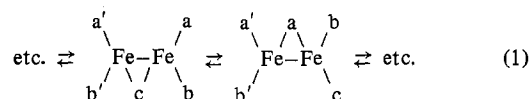
^a The form of the anisotropic thermal parameter is $\exp[-(\beta_{11}h^2 + \beta_{22}k^2 + \beta_{33}l^2 + \beta_{12}hk + \beta_{13}hl + \beta_{23}kl)]$.

observed that the Cr-P bond length in the latter compound is 0.11 Å shorter than in the former compound. A very similar difference is observed here. The di(tertiary phosphite) POP in **1** forms Fe-P bonds whose mean length, 2.151 (7) Å, is 0.10 Å shorter than the average Fe-P bond in the di(tertiary phosphine) complex $(\text{Ph}_2\text{PCH}_2\text{PPh}_2)\text{Fe}_2(\text{CO})_7$.

A slight shortening of the mean Fe-CO terminal distance in **1** compared to $(\text{Ph}_2\text{PCH}_2\text{PPh}_2)\text{Fe}_2(\text{CO})_7$ is also observed. The mean Fe-CO terminal distances are 1.70 (2) and 1.79 (2) Å in the phosphite and phosphine compounds, respectively. This may well reflect the increased level of substitution of CO groups by phosphorus ligands in the former. In fact the mean Fe-CO distance observed here is among the shortest ever reported.

Fluxional Behavior of 1 and 2. The low-temperature limiting spectrum for **1** at -158 °C (Figure 2) is consistent with its structure in the crystal. The bridging carbonyl resonance at 280.0 ppm shows a quintet pattern ($J_{13\text{C}-31\text{P}} = 18.9$ Hz) attributable to coupling with four equivalent phosphorus atoms, while the two terminal carbonyl resonances, at 221.3 and 215.7

ppm, show triplet patterns ($J_{13\text{C}-31\text{P}} = 14.8$ and 23.3 Hz, respectively). Assignment of the spectrum at -158 °C can be made unambiguously from its behavior as the temperature is raised. From -158 to -112 °C the resonance at 221.3 ppm broadens more rapidly than the resonance at 215.7 ppm, although all five carbonyls are being scrambled by the same process. This is what would be expected in terms of the process shown in eq 1. As noted previously in our report³ on



$(1,2\text{-C}_4\text{H}_4\text{N}_2)\text{Fe}_2(\text{CO})_7$, for such a process the resonance for the a,a' pair of CO's should broaden twice as fast as that for the b,b' pair since in each step one of b,b' pair remains in the same environment, while both a and a' change. Thus, the following assignment can be made: C(3)-O(3), 280.0 ppm; C(4)-O(4), C(7)-O(7), 215.7 ppm; C(5)-O(5), C(6)-O(6), 221.3 ppm.

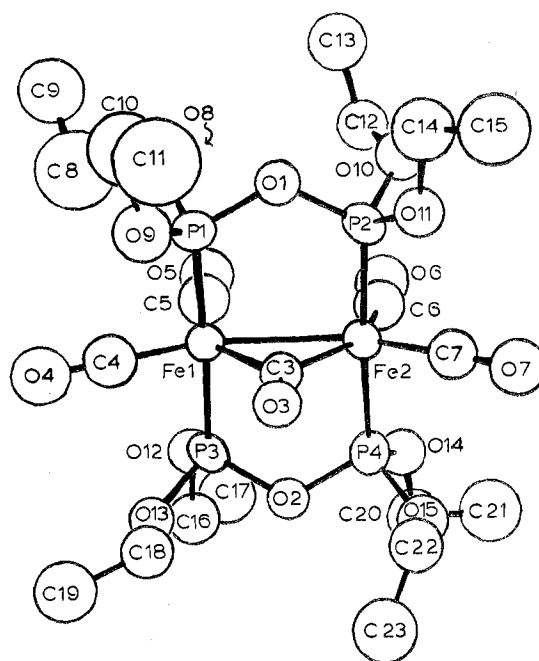
Table II. Bond Lengths (Å) in $(\text{POP})_2\text{Fe}_2(\text{CO})_5$

	Molecule 1	Molecule 2
Fe(1)-Fe(2)	2.663 (2)	2.669 (2)
-P(1)	2.154 (4)	2.160 (4)
-P(3)	2.149 (4)	2.155 (4)
-C(3)	1.912 (15)	1.928 (11)
-C(4)	1.692 (13)	1.685 (14)
-C(5)	1.712 (23)	1.736 (14)
Fe(2)-P(2)	2.150 (4)	2.148 (5)
-P(4)	2.134 (4)	2.158 (4)
-C(3)	1.920 (12)	1.947 (10)
-C(6)	1.705 (21)	1.732 (13)
-C(7)	1.677 (18)	1.697 (14)
P(1)-O(1)	1.643 (8)	1.613 (9)
-O(8)	1.590 (10)	1.636 (9)
-O(9)	1.587 (10)	1.573 (11)
P(2)-O(1)	1.615 (8)	1.634 (8)
-O(10)	1.584 (9)	1.580 (10)
-O(11)	1.580 (10)	1.601 (12)
P(3)-O(2)	1.607 (8)	1.644 (7)
-O(12)	1.569 (12)	1.585 (9)
-O(13)	1.607 (8)	1.592 (8)
P(4)-O(2)	1.628 (8)	1.654 (8)
-O(14)	1.580 (12)	1.568 (7)
-O(15)	1.602 (11)	1.600 (8)
C(3)-O(3)	1.205 (14)	1.213 (11)
C(4)-O(4)	1.174 (13)	1.205 (14)
C(5)-O(5)	1.202 (19)	1.175 (13)
C(6)-O(6)	1.183 (19)	1.192 (13)
C(7)-O(7)	1.188 (17)	1.192 (15)
O(8)-C(8)	1.477 (18)	1.542 (19)
O(9)-C(10)	1.417 (16)	1.212 (20)
O(10)-C(12)	1.515 (16)	1.546 (21)
O(11)-C(14)	1.495 (16)	1.343 (28)
O(12)-C(16)	1.421 (16)	1.459 (13)
O(13)-C(18)	1.469 (16)	1.467 (17)
O(14)-C(20)	1.475 (27)	1.511 (16)
O(15)-C(22)	1.564 (20)	1.466 (14)
C(8)-C(9)	1.512 (25)	1.587 (28)
C(10)-C(11)	1.500 (20)	1.559 (19)
C(12)-C(13)	1.452 (23)	1.476 (19)
C(14)-C(15)	1.463 (20)	1.440 (23)
C(16)-C(17)	1.549 (19)	1.548 (17)
C(18)-C(19)	1.452 (20)	1.448 (21)
C(20)-C(21)	1.511 (27)	1.354 (38)
C(22)-C(23)	1.328 (26)	1.377 (22)

Because of the overlap of signals in the terminal CO region, the spectra for **2** (Figure 3) cannot be analyzed in as much detail. In the limiting spectrum at -149°C the poorly resolved triplet at 260.3 ppm is assigned to the bridging carbonyl. The remaining six terminal carbonyl groups all give signals near 214.3 ppm resulting in an irregular multiplet. As the temperature is raised, it is evident that there are two scrambling processes. First, from -149 to -108°C the bridging CO and apparently four terminal CO's begin to scramble. Coalescence occurs at about -108°C . This process is presumably identical with that observed in **1** although that conclusion is not completely clear from the spectra. Above -108°C all resonances become or remain broad until and above about -80°C , where they coalesce and eventually sharpen to a very closely spaced triplet. This second exchange process is most probably one of local exchange within each $\text{Fe}(\text{CO})_3$ moiety. These local exchanges coupled with the already rapid internuclear exchange process result in rapid scrambling of all seven carbonyl ligands.

Activation parameters were not obtainable for **1** and **2** because of the relatively poor quality of the spectra. The coalescence temperatures in **1**, **2**, and $(1,2\text{-C}_4\text{H}_4\text{N}_2)\text{Fe}_2(\text{CO})_7$ for the internuclear process are very similar, viz., ~ -90 , ~ -108 , and $\sim -96^\circ\text{C}$, respectively.

It is clear that the rate of the internuclear, cyclic exchange process is not very sensitive to the Fe-Fe bond length, since compound **1**, $(1,2\text{-C}_4\text{H}_4\text{N}_2)\text{Fe}_2(\text{CO})_7$, and $(\text{Ph}_2\text{PCH}_2\text{PPh}_2)\text{-}$

**Figure 1.** ORTEP drawing showing the molecular structure of $[(\text{EtO})_2\text{POP}(\text{OEt})_2]_2\text{Fe}_2(\text{CO})_5$, **1**, and defining the atomic numbering scheme for Tables I-IV.**Table III.** Selected Bond Angles (deg) in $(\text{POP})_2\text{Fe}_2(\text{CO})_5$

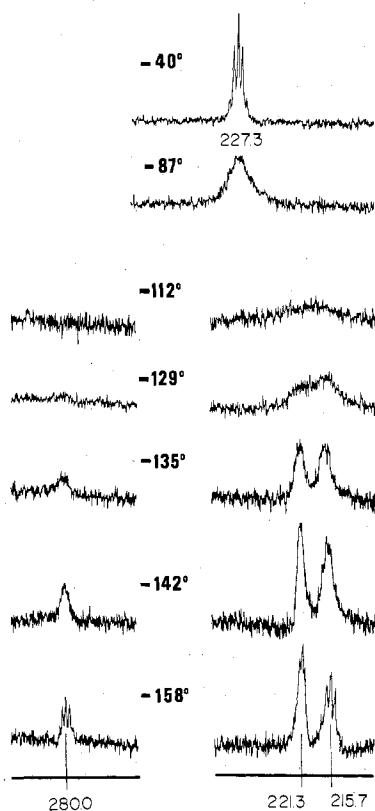
	Molecule 1	Molecule 2
Fe(2)-Fe(1)-P(1)	92.64 (12)	90.28 (12)
-P(3)	91.48 (11)	92.79 (11)
-C(3)	46.10 (36)	46.75 (31)
-C(4)	152.85 (54)	153.73 (47)
-C(5)	100.40 (52)	98.18 (43)
Fe(1)-Fe(2)-P(2)	91.24 (12)	93.48 (12)
-P(4)	92.10 (12)	91.68 (12)
-C(3)	45.87 (45)	46.18 (33)
-C(6)	94.72 (54)	93.57 (42)
-C(7)	156.62 (54)	157.51 (43)
P(1)-Fe(1)-P(3)	173.51 (16)	175.70 (15)
P(2)-Fe(2)-P(4)	173.17 (22)	172.05 (16)
C(3)-Fe(1)-C(4)	106.76 (64)	107.05 (54)
C(3)-Fe(1)-C(5)	146.47 (62)	144.70 (52)
C(4)-Fe(1)-C(5)	106.75 (75)	108.09 (63)
C(3)-Fe(2)-C(6)	140.46 (71)	139.75 (53)
C(3)-Fe(2)-C(7)	110.77 (71)	111.35 (54)
C(6)-Fe(2)-C(7)	108.65 (77)	108.90 (59)
Fe(1)-P(1)-O(1)	115.79 (30)	118.12 (33)
-P(1)-O(8)	112.87 (44)	115.07 (45)
-P(1)-O(9)	123.74 (37)	122.96 (49)
O(1)-P(1)-O(8)	104.22 (46)	100.45 (49)
O(1)-P(1)-O(9)	99.30 (51)	99.16 (59)
O(8)-P(1)-O(9)	97.89 (53)	96.80 (55)
Fe(2)-P(2)-O(1)	117.13 (31)	115.83 (42)
-O(10)	114.98 (40)	115.53 (45)
-O(11)	119.74 (35)	120.25 (44)
O(1)-P(2)-O(10)	103.70 (44)	102.27 (45)
O(1)-P(2)-O(11)	97.70 (47)	100.25 (52)
O(10)-P(2)-O(11)	100.64 (51)	99.76 (65)
P(1)-O(1)-P(2)	119.31 (51)	120.47 (59)
Fe(1)-C(3)-Fe(2)	88.03 (65)	87.07 (44)
Fe(1)-C(3)-O(3)	136.95 (92)	138.02 (85)
Fe(1)-C(4)-O(4)	178.19 (1.35)	178.52 (1.19)
Fe(1)-C(5)-O(5)	173.26 (1.42)	175.93 (1.27)
Fe(2)-C(6)-O(6)	175.64 (1.40)	178.16 (1.39)
Fe(2)-C(7)-O(7)	178.89 (1.49)	179.70 (1.03)

$\text{Fe}_2(\text{CO})_7$ have Fe-Fe bond lengths of 2.666 (2), 2.573 (1), and 2.709 (2) Å, respectively. The molecule with the longest Fe-Fe bond length, $(\text{Ph}_2\text{PCH}_2\text{PPh}_2)\text{Fe}_2(\text{CO})_7$, undergoes carbonyl exchange with the greatest ease; for this molecule no broadening in the carbon-13 NMR spectrum was observed down to -100°C .

Table IV

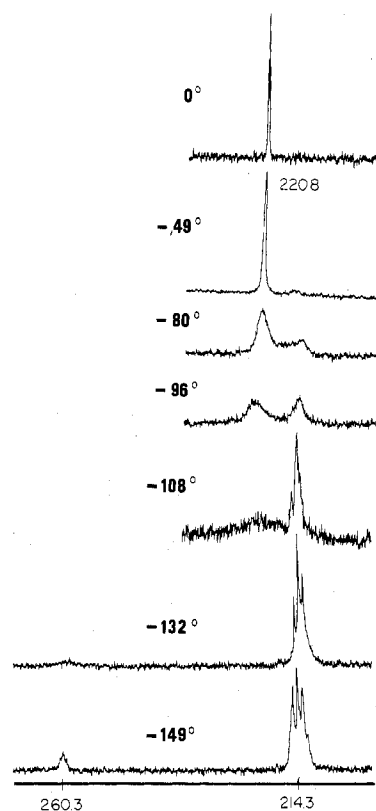
Least-Squares Planes for 1							
Plane	Atoms defining plane		Equation of plane ^a				
I	Fe(1), Fe(2), P(1), P(2), P(3), P(4)		-0.8530x - 0.0008y - 0.5219z = -12.3597				
II	Fe(1), Fe(2), C(3), C(4), C(5), C(6), C(7)		0.3785x - 0.7066y - 0.5979z = -0.9469				
Displacement of Atoms from Mean Plane (A)							
Plane I			Plane II				
Fe(1)	-0.063	P(2)	-0.036	Fe(1)	-0.003	C(5)	-0.069
Fe(2)	-0.074	P(3)	-0.041	Fe(2)	-0.012	C(6)	0.077
P(1)	0.104	P(4)	0.110	C(3)	0.009	C(7)	-0.038
				C(4)	0.037		

Dihedral Angle I-II: 89.4°

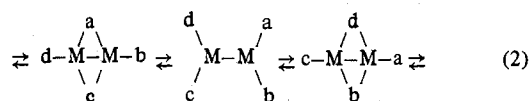
^a Equations have the form $Ax + By + Cz = D$, where x , y , and z are fractional monoclinic coordinates.Figure 2. Carbon-13 NMR spectra for $[(\text{EtO})_2\text{POP}(\text{OEt})_2]_2\text{Fe}_2(\text{CO})_5$, 1, at various temperatures. Chemical shifts are in ppm from Me_4Si .

In conclusion, it is pertinent to point out that the geometrically cyclic intermolecular exchange process that occurs in the binuclear systems just discussed can be regarded as only one type among a series of similar ones, all of which are describable as mathematically cyclic permutations. If a bi- or polynuclear molecule contains a set of n CO groups, these may be listed as a vector $\{\text{CO}_1, \text{CO}_2, \dots, \text{CO}_n\}$ and each step in the scrambling process can be represented by the operation upon that vector of a matrix of the following type, depending on the direction of cycling.

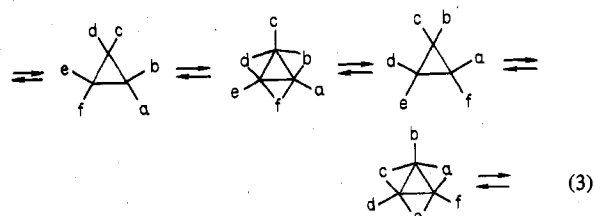
$$\begin{bmatrix} 0 & 0 & 0 & \dots & 0 & 1 \\ 1 & 0 & 0 & \dots & 0 & 0 \\ 0 & 1 & 0 & \dots & 0 & 0 \\ \dots & \dots & \dots & \dots & \dots & \dots \\ 0 & 0 & 0 & \dots & 1 & 0 \end{bmatrix} \quad \text{or} \quad \begin{bmatrix} 0 & 1 & 0 & \dots & 0 & 0 \\ 0 & 0 & 1 & \dots & 0 & 0 \\ \dots & \dots & \dots & \dots & \dots & \dots \\ 0 & 0 & 0 & \dots & 0 & 1 \\ 1 & 0 & 0 & \dots & 0 & 0 \end{bmatrix}$$

Figure 3. Carbon-13 NMR spectra for $[(\text{EtO})_2\text{POP}(\text{OEt})_2]_2\text{Fe}_2(\text{CO})_7$, 2, at various temperatures. Chemical shifts are in ppm from Me_4Si .

Actually, the system in which internuclear scrambling of CO groups was first discovered,⁷ $(\eta^5\text{-C}_5\text{H}_5)\text{Fe}(\text{CO})(\mu\text{-CO})_2\text{Fe}(\text{CO})(\eta^5\text{-C}_5\text{H}_5)$, can be considered as another example of this type of process in which there are two metal atoms and four CO groups, and eq 2 expresses the essence of what happens.



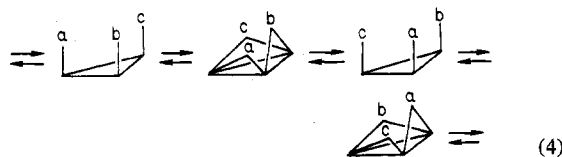
Several cases, differing in their structural details, in which $n = 6$ and the set of metal atoms is an equilateral triangle have already been reported. For example, in $(1,2\text{-C}_4\text{H}_4\text{N}_2)\text{-Os}_3(\text{CO})_{10}$ there are six terminal CO groups in the Os_3 plane, two on each metal atom. At temperatures of -30°C and below these scramble⁸ by a process believed to be that shown in eq 3, in which the bridged structures are less stable tau-



omeric intermediates. In $(1,2\text{-C}_4\text{H}_4\text{N}_2)\text{Ru}_3(\text{CO})_{10}$, on the other hand, the bridged structure is the more stable one and the nonbridged structures are the tautomeric intermediates⁹ through which the cyclic scrambling process proceeds.

There are also several examples of three CO groups scrambling over a triangular set of three metal atoms. For example, in the C_{3v} isomer of $(\eta^5\text{-C}_5\text{H}_5)_3\text{Rh}_3(\text{CO})_3$ ¹⁰ and in $(\text{Ph}_2\text{PCH}_2\text{PPh}_2)\text{Ru}_2(\text{CO})_{10}$ ¹¹ the process proceeds according to eq 4, with the bridged form being the stable one in the

former case and the nonbridged form being the more stable in the latter.



There is no reason, in principle, such cyclic scrambling processes may not occur in cases where even larger numbers, x , of metal atoms constitute the fixed skeleton around which the x , $2x$, or other $>x$ CO groups move cyclically. Nor is there any requirement that the set of x metal atoms and/or the set of CO groups be geometrically planar. There is only the topological requirement that the set be continuous and closed. It should also be stressed that the existence of such a continuous, closed loop is only a necessary condition but not a sufficient condition for cyclic scrambling to occur.

All processes in this general class share the characteristic that as they proceed they can continuously maintain the electronic population of each metal atom at its optimum value. This is basically because both terminal and bridging CO ligands contribute two electrons to the metal atoms, and in

all these processes the breaking of some CO bonds and formation of new ones always occur in a compensatory way.

Acknowledgment. We thank the Robert A. Welch Foundation for support under Grant No. A-494.

Registry No. 1, 65255-73-4; 2, 65255-85-8; ^{13}C , 14762-74-4.

Supplementary Material Available: A table of calculated and observed structure factors (14 pages). Ordering information is given on any current masthead page.

References and Notes

- (1) (a) Texas A&M University. (b) University of Natal.
- (2) F. A. Cotton and J. M. Troup, *J. Am. Chem. Soc.*, **96**, 4422 (1974).
- (3) F. A. Cotton, B. E. Hanson, J. D. Jamerson, and B. R. Stults, *J. Am. Chem. Soc.*, **99**, 3293 (1977).
- (4) A. L. DuPreez, I. L. Marais, R. J. Haines, A. Pidcock, and M. Safari, *J. Organomet. Chem.*, **141**, C10 (1977).
- (5) All computations were performed at the Molecular Structure Corp., College Station, Tex. 77840.
- (6) H. J. Plastas, J. M. Stewart, and S. O. Grim, *Inorg. Chem.*, **12**, 265 (1973).
- (7) R. D. Adams and F. A. Cotton, *J. Am. Chem. Soc.*, **92**, 5003 (1970); **95**, 6589 (1973); O. A. Gansow, A. R. Burke, and W. D. Vernon, *ibid.*, **94**, 2550 (1972).
- (8) F. A. Cotton and B. E. Hanson, *Inorg. Chem.*, **16**, 2820 (1977).
- (9) F. A. Cotton, B. E. Hanson, and J. D. Jamerson, *J. Am. Chem. Soc.*, **99**, 6588 (1977).
- (10) R. J. Lawson and J. R. Shapley, *J. Am. Chem. Soc.*, **98**, 7433 (1976).
- (11) F. A. Cotton and B. E. Hanson, *Inorg. Chem.*, **16**, 3369 (1977).

Contribution from the Department of Chemistry,
Texas A&M University, College Station, Texas 77843

An Exceedingly Short Metal–Metal Bond in a Bis(*o*-alkoxyphenyl)dicarboxylatodichromium Compound

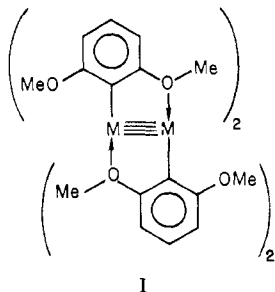
F. ALBERT COTTON* and MICHELLE MILLAR

Received December 7, 1977

To gain more information on the ability of *o*-oxyphenyl type ligands to promote the formation of exceedingly short metal–metal bonds, a compound containing only two such ligands, viz., *o*-*tert*-butoxyphenyl, together with two acetato groups, has been synthesized and structurally characterized by X-ray crystallography. The molecule, $\text{Cr}_2(\text{o-Bu}^t\text{OC}_6\text{H}_4)_2(\text{O}_2\text{CCH}_3)_2$, has virtual C_{2h} symmetry, the mirror plane coinciding with the mean plane of the *o*- OC_6H_4 ligands. The molecule has a rigorous crystallographic inversion center. Even with only two *o*-oxyphenyl type ligands, the Cr–Cr quadruple bond is still extremely short, 1.862 (1) Å, though slightly (~ 0.02 Å) longer than those found in compounds containing only *o*-oxyphenyl type ligands. The basic crystallographic data are as follows: space group $P2_1/c$, $a = 8.917$ (2) Å, $b = 18.926$ (4) Å, $c = 8.232$ (2) Å, $\beta = 116.32$ (1)°, $V = 1245.2$ (5) Å³, $Z = 2$. A total of 1814 independent observations with $I > 3\sigma(I)$ has been used to refine the structure to $R_1 = 0.056$ and $R_2 = 0.090$. Other important dimensions are Cr–C = 2.064 (3) Å, Cr–OBU^t = 2.118 (2) Å, Cr–O(acetate) = 1.995 (2) and 1.996 (2) Å, and $\angle\text{Cr–Cr–C} = 90.5$ (1)°.

Introduction

The surprising discovery that the compounds $\text{Cr}_2(\text{DMP})_4$ and $\text{Mo}_2(\text{DMP})_4$, where DMP represents 2,6-dimethoxyphenyl, which have the qualitatively expected structure I,



contain the shortest known Cr–Cr and Mo–Mo quadruple bonds¹ was recently reported, and for chromium, essentially the same Cr–Cr distance was also found² in tetrakis(2,4,6-trimethoxyphenyl)dichromium. These two Cr–Cr distances,

1.847 (1) and 1.849 (2) Å, are considerably shorter than the shortest ones accurately known before that, namely, those in $\text{Cr}_2(\text{CH}_3)_8^{4-}$, 1.980 (5) Å,³ and $\text{Cr}_2(\text{C}_4\text{H}_8)_4^{4-}$, 1.975 (5) Å.⁴ They are far shorter than those in $\text{Cr}_2(\text{O}_2\text{CX})_4$ species in which X may be R, Ar, O, or OR, which range from 2.21 to 2.54 Å.⁵ More recently, an even shorter Cr–Cr distance, 1.830 (4) Å, was found in $\text{Li}_6\text{Br}_2(\text{Et}_2\text{O})_6[\text{Cr}_2(\text{o-OC}_6\text{H}_4)_4]$.⁶

Among the many questions prompted by these discoveries, we deal in this paper with that concerning the bond distance which will result when the ligand set consists of a mixture of the *o*-oxyphenyl type ligand and the O_2CX type. We have found a way to synthesize such a molecule and have determined its structure. The synthesis was designed on the principle that for a ligand of type II, the presence of a suf-

